In Situ Formation of Carbon Nanotubes Encapsulated within Boron Nitride Nanotubes *via* Electron Irradiation

Raul Arenal[†,‡,⊥,*] and Alejandro Lopez-Bezanilla[§,⊥]

[†]Laboratorio de Microscopias Avanzadas (LMA), Instituto de Nanociencia de Aragon (INA), Universidad de Zaragoza, C/Mariano Esquillor, 50018 Zaragoza, Spain, [‡]Fundation ARAID, 50018 Zaragoza, Spain, and [§]Materials Science Division, Argonne National Laboratory, 9700 South Cass Avenue, Lemont, Illinois 60439, United States. [⊥]Both authors have contributed equally to this work.

ABSTRACT We report experimental evidence of the formation by *in situ* electron-irradiation of single-walled carbon nanotubes (C-NT) confined within boron nitride nanotubes (BN-NT). The electron radiation stemming from the microscope supplies the energy required by the amorphous carbonaceous structures to crystallize in a tubular form in a catalyst-free procedure, at room temperature and high vacuum. The structural defects resulting from the interaction of the shapeless carbon with the BN nanotube are corrected in a self-healing process throughout the crystallinization. Structural changes developed during the irradiation process such as defects formation and evolution, shrinkage, and shortness of the BN-NT were *in situ* monitored. The outer BN wall provides a protective and insulating shell against environmental perturbations to the inner C-NT without affecting their electronic properties, as demonstrated by first-principles calculations.

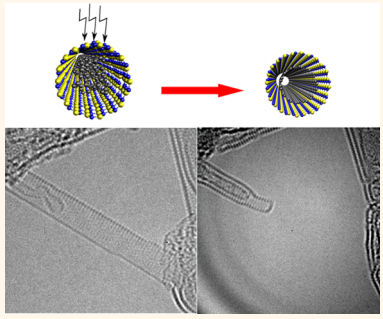

KEYWORDS: hybrid (boron nitride carbon) nanotubes · HRTEM · electron-irradiation · EELS-STEM · DFT calculations

The controlled synthesis and growth of carbon nanotubes (C-NTs) has been a long-standing challenge in the fabrication of carbon-based materials for electronic applications. The successful integration of C-NTs on electronic devices is allowing for the design and construction of ultrasmall transistors able to conduct high density electric charge in low-diameter channels.[1] However, as many studies have demonstrated, the perturbation of the graphitic network of single- and multiwalled nanotubes represents a drawback for the implantation of C-NTs as the fundamental building block of high performance transisvtors. Indeed, geometrical distortions (nanotube bends), structural defects (vacancies, Stone–Wales defects), and physi- and chemi-sorption of external molecules inevitably lead to a severe diminution of the nanotube electronic properties that may result on a full suppression of its conductance ability.[2] It is therefore necessary to develop experimental strategies for C-NT synthesis that guarantee the formation of crystalline structures of carbon materials while ensuring a protection from the environment without affecting their electronic properties. Under this context, owing to the uniform electronic properties and chemical inertness characteristics of boron nitride (BN),[3,6,8] BN nanotubes (BN-NTs) may team up with C-NTs in the realization of hybrid-structures for achieving these goals. Indeed, BN-NTs are resistive to oxidation up to 900 °C, transparent to visible-near UV light, and possess a high resistance to irradiation. This makes BN-NTs ideal candidates for insulating, transparent, and anticorrosive coatings under extreme thermal and chemical conditions.[3−8] BN-NTs and C-NTs are isomorphs with a hexagonal lattice that can be arranged on concentric layers. Although the 3 atoms can mix in a same layer, B and N atoms are usually present in 1:1 ratio and preferably in independent layers or patches to reduce the interface BN-C energy.[3,6,8−10] Both kinds of nanotubes possess similar mechanical properties such as a great stiffness (the Young's

* Address correspondence to arenal@unizar.es.

Received for review May 28, 2014 and accepted July 25, 2014.

Published online July 25, 2014
10.1021/nn502912w

modulus of single-walled BN-NT has been estimated to be as high as 1.11 TPa, similar to that of single-walled C-NT).[11,31] One of the major differences between both types of tubes is the electronic properties[3,4,6,8,12−14] The pure covalent C−C bond and the hyperconjugation of the π-orbital network yield C-NTs an either small-gap semiconducting or metallic material depending on the tube chirality. On the contrary, the high ionic character of the BN bond confers to any kind of BN-NT an insulating behavior with a band gap measured as ≈6 eV.[3,6,12,13] The combination of both C and BN materials in a hybrid structure may lead to the development of nanostructures (NS) that could circumvent some of the limitations of C-NTs for electronic applications.

In the last 15 years, the ability and usefulness of electron-irradiation treatments for modifying the behavior of nanomaterials under extreme conditions and radiation has been widely demonstrated.[15,31] Irradiating C and BN nanotubes with energetic electrons is an appealing technique for manufacturing and engineering materials at the nanoscale. Numerous previous works have evidenced the applicability of electron-irradiation treatments such as welding to form molecular junctions,[16] coalescence[17] and growth of NT,[18] phase transformation of solid Mg oxides filled BN-NT,[20] and transformation of fullerenes filling BN-MWNT into C-NT,[19] and in other forms of carbon materials, as the crystallization/graphitization of amorphous carbon on h-BN substrates[22] and restructuration of graphene's grain boundaries.[23]

In this paper, we report the formation *via* electron-irradiation of crystalline carbon nanotubes encapsulated in larger diameter boron nitride nanotubes. *In situ* electron-irradiation in a transmission electron microscope (TEM) allowed us to monitor and investigate the structural evolution of BN-SWNT under high-energy beam radiation simultaneously to the formation process of crystalline hybrid C nanostructures from amorphous materials. The resulting C-NT remains stable and encapsulated within the outer BN tube, which provides a protective shell against environment perturbations. First-principles simulations of the electronic structure of the concentric tubular materials demonstrate that the original hyperconjugated network of the inner C-NT electronic states is barely affected by the outer BN shell.

RESULTS

The collected synthesis products have been studied by high resolution (HRTEM) imaging and spatial-resolved electron energy loss spectroscopy (SR-EELS). As we proceeded in a previous work,[24] some of the (double-walled (DW) and single-walled (SW)) tubes were filled with amorphous carbon as displayed in the bright field and high angle annular dark field (HAADF) scanning TEM (STEM) images of Figure 1a,b

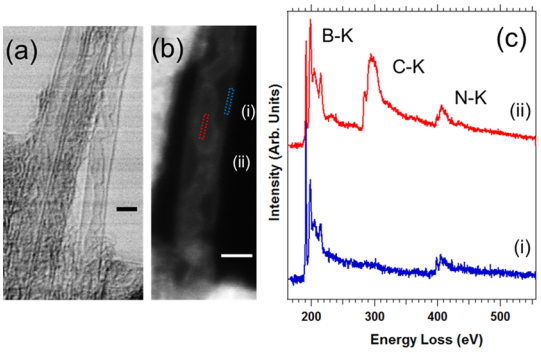

Figure 1. Bright field and HAADF images of (a) a bundle of 2 DW and (b) individual SW BN-NTs. An EELS-SPIM was recorded on the individual BN-SWNT on the right of (a). (c) Fourteen EEL spectra, selected from the SPIM in each of the rectangular areas marked in blue (i) and in red (ii) in the HAADF-STEM image (b), were added after background subtraction. B−K and N−K edges are displayed in (i) and (ii), while C−K edge is only displayed in (ii). All scale bars are 2 nm.

where a disordered carbonaceous nanostructure (NS) is visible. To better characterize these nanotubes, we have developed SR-EELS-STEM analyses with high spatial resolution <2 Å. An EELS spectrum-image (SPIM) was recorded on a partially filled individual BN-SWNT, see Figure 1b. After background subtraction, 14 EEL spectra were selected from the SPIM in each of the rectangular areas marked in blue (i) and in red (ii) in Figure 1b. B−K and N−K edges are visible in the EEL spectrum of Figure 1c-i, after background subtraction. The fine structures near the edge (ELNES) confirms that the atoms of the BN tubes are sp^2 bonded with a 1:1 B to N ratio. However, in the EEL spectrum of Figure 1c-ii, the C−K edge is also present. From the ELNES analysis of this C−K edge, we conclude that it corresponds to amorphous carbon filling the BN tube. The origin of this C comes from the h-BN target used for the synthesis of these materials and the filling mechanism is described elsewhere.[24]

In Figure 2, an eight-frame HRTEM image sequence (see Material and Methods section for details concerning the acquisition) shows the evolution toward a nanotube geometry of a disordered C nanostructure enclosed within a BN-NT. The HRTEM micrographs depicted in this image sequence have been selected from those displayed in the Video S1 (Supporting Information), which corresponds to the whole irradiation process. The electron-irradiation process occurs for a total cumulative dose of up to 1.8×10^7 e−/Å^2 and over a period of 380 s at room temperature. In the HRTEM sequence defined by red arrows, a disordered carbonaceous nanostructure is first observed inside a straight BN-NT and evolves over time to a crystalline tubular structure. The crystalline quality of these hybrid double-walled NT is visible in Figure 2g,h and from Figure S1 (Supporting Information). Simultaneously, a gradual shrinkage and a reshaping of the BN-NT are observed. As a consequence of both processes, the

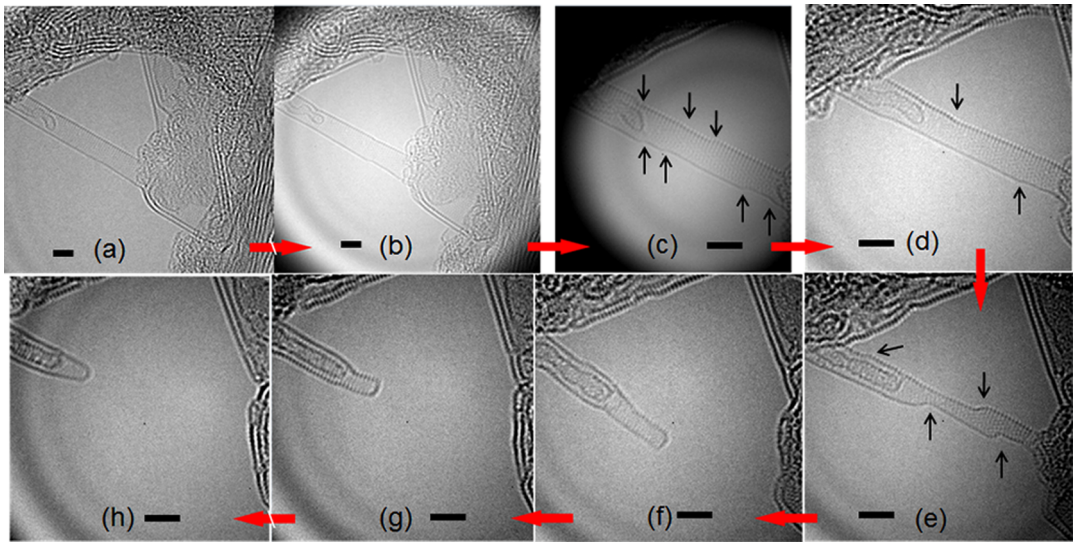

Figure 2. Eight-frame sequence of HRTEM images displaying the formation process of a crystalline C-NT from disordered-amorphous-like carbonaceous nanostructure encapsulated in a BN-NT under TEM radiation exposure. The black arrows on these images mark the presence of kinks. All scale bars are 2 nm.

nanotube eventually breaks. In addition, the formation of an atomic-scale bridge between the tip of the carbon nanostructure and the outer BN wall, and the subsequent reparation of the defect on both materials, is also observed.

Recently, we demonstrated that ion-irradiation processes of these nanomaterials are most of all dominated by their nanostructured character.[7] The transformations of the two BN and C nanostructures are intimately related to (i) their different electronic properties, namely, BN is an insulator and C a conductor; (ii) their elemental composition and behavior under electron-irradiation; (iii) their spatial distribution, which allows the outer BN tube to provide a protective cage for the inner C atoms, and to the latter to act as structural "reinforcers"/stabilizers for the BN-NTs.

Due to the differences in the electronic structures of both NS, a completely different behavior and stability under the electron beam is expected. For an insulating material with localized electrons, the irradiation with energetic electrons may lead to bond breaking, ionization, and structural damage. On the contrary, the delocalized conduction electrons of a metal allow for the quenching of the electronic excitations[15,31] and the subsequent structural damage restructuration. In the case of good heat and charge conductor sp^2 carbon materials, the irradiation's processes are mainly governed by ballistic knock-on atomic displacements.

On the other hand, the electron knock-on damage thresholds of BN-NT and amorphous C are different, albeit they are both low-dimensional light-elements based materials. The electron knock-on damage threshold of both BN-NTs and amorphous C is lower than that of a free-standing C-NT (≈86 keV)[21,22,25,26] Zobelli *et al.* calculated the response of the system to irradiation or emission energy threshold (T_d) (also referred as to threshold displacement energy for the an atom) of B and N in BN sheets as $T_{d-N} = 14$ eV and $T_{d-B} = 15$ eV, and for C in a graphene sheet $T_{d-C-graphene} = 23$ eV, indicating that BN sheets are less stable under electron-irradiation than graphene. In fact, an incident electron energy of 74 keV corresponds to a maximum energy transfer of 15 eV for a B atom in a h-BN sheet satisfying the emission conditions. In the case of N emission, the incident electron energy should be at least of 84 keV. Therefore, under our experimental conditions of 80 keV, B atoms can be ejected. Since the C nanostructure is enclosed in the BN-NT container, both the irradiation process and the electron knock-on damage threshold differ from the one of the unprotected NS.

We move on to the description of the events observed and to the discussion of the mechanisms and processes underlying the electrons' interaction with the nanostructures. During the first stages of the electron-irradiation process, the more greatly marked event is the BN-NT's diameter shrinking, which occurs throughout the irradiation experiment. The diameter decreases from 2 to 1.6 nm. This shrinkage is produced by a combination of sputtering (atomic knock to vacuum), reconstruction, and defects formation and migration. The formation of kinks and their displacement along the NT side-walls are shown in Figure 2 (marked with black arrows) and in the Video S1 (provided in Supporting Information). As Zobelli *et al.* pointed out,[27] these types of kinks are due to the formation of extended defects which can be ascribed to the formation of dislocations upon sequential ejection of adjacent atoms. The kinks' migration are at the origin of the NT chiral angle modification which randomly varies from 5.2° to 10.2° (see Figure 3).

Simultaneously to the BN-SWNT narrowing, the restructuration of the disordered carbonaceous NS inside

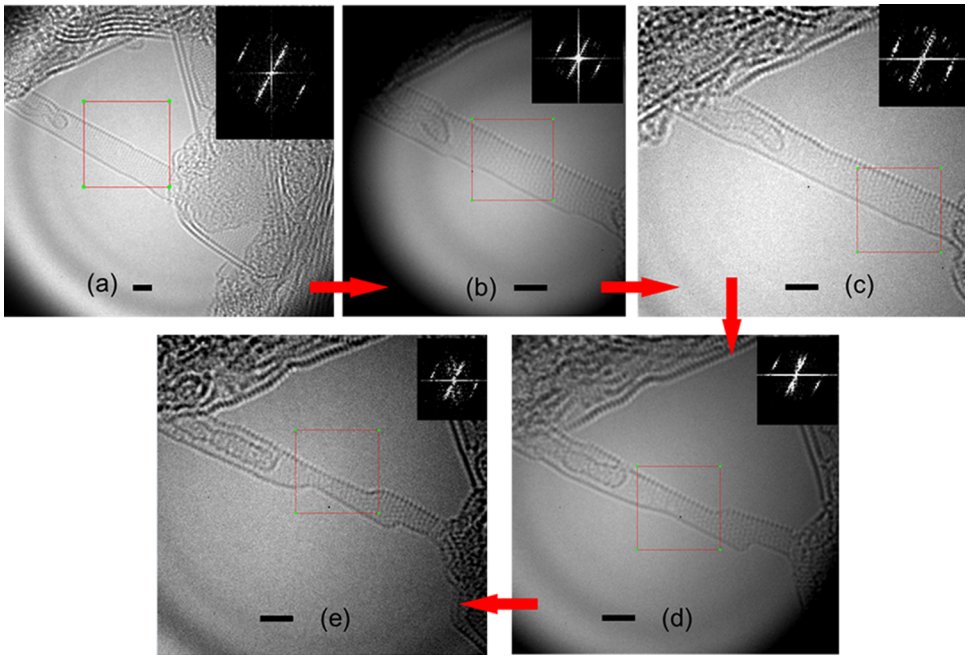

Figure 3. Five-frame HRTEM sequence displaying a BN-NT chiral angle modification during the electron-irradiation process. In inset, the Fourier transform (FT) of the area selected in each of these micrographs. The chiral angle measured in each FT is (a) 5.8°, (b) 8.9°, (c) 8.2°, (d) 6.2°, and (e) 10.2°.

the NT is observed. Along this process, the BN-NT plays a twofold role: as protective cage during the irradiation and as a template for the morphological reorganization of the C material. It is important to emphasize that this reorganization is catalyst-free, since no metal nanoparticles were used for the synthesis of the BN-NT.[24,28] The restructuration is mainly due to atomic displacements and reconstruction of structural damage under the electron beam, as can be followed in Supporting Information Video S1. No significant change in the dimension of the carbon NS was observed even when some carbon atoms were ejected or migrated to the walls of the BN-NT. The length of the carbon nanostructure was fairly uniform at ≈4.1 nm. Only the carbon nanostructure width was slightly modified from 0.67 nm at the thinnest to 0.94 nm at the largest areas (see Figure 2a). At the end of the irradiation process, the diameter of the C-NT was kept uniform, 0.85 nm (Figure 2g or h). The bright spots displayed are interpreted as the signature of point defects whose propagation contributes to the restructuration process of the amorphous C. These reconstruction mechanisms are related to thermally activated migration-mediated self-healing. However, the encapsulation of C within a BN-NT was observed to follow different behaviors depending on the carbon density. Indeed, the geometry of the initially shapeless C can either crystallize in a tubular form or remain amorphous. Figure 4a shows a HRTEM image of a BN-DWNT containing an indistinct mass of C. The nanotubes are terminated with a flat cap exhibiting an opening (red circle) through which the encapsulated C drains out. A different behavior was found on low

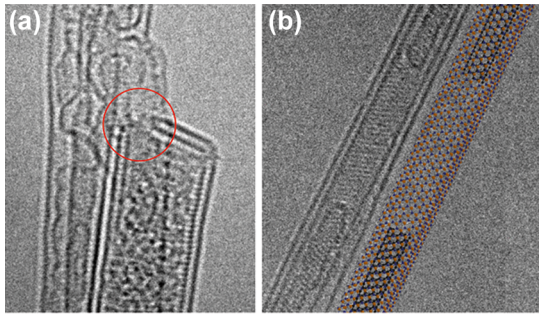

Figure 4. (a) Amorphous C flowing out of a double-walled BN nanotube through an opening at the nanotube cap. (b) Two capped single-walled C-NT encapsulated within a double-walled BN-NT. The schematic representation models the HRTEM image.

concentrations of C within a BN-DWNT under external radiation. Figure 4b shows an image of two capped single-walled C-NT enclosed within a double-walled BN-NT. From this HRTEM image, the diameter of the inner C-NT was estimated to be of ≈1 nm. The ball-and-stick model besides represents a structural model of the real image. As schematized on the right of Figure 4b, the crystalline carbon structure is formed as a result of the atomic rearrangement of initially disorder carbonaceous structure in a catalyst-free process driven by the external TEM irradiation.

After the initial shrinkage of the NT, the second event that we observed was the cut of the BN-NT. In the case of BN-MWNT, the electron-irradiation induced cut was accompanied by the formation of nanoarches,[29] pointing out that the mechanism behind the cutting of a single-walled BN-NT may be different

as we do not observe this arches' formation. Indeed, the clean cut of the BN-SWNT can be ascribed to pressure-effects related dynamics phenomena. Sun *et al.*[30] and Banhart *et al.*[31] demonstrated that electron-irradiation on NT may lead to extreme pressures (in the order of tens of GPa), which can yield the NT's collapse and cut.[15] This cut occurs when the diameter of the NT is close to the lowest limit of structural stability of ≈0.4 nm. As observed in Supporting Information Video S1, after the NT is broken a reconstruction at the open tip in the form of a flat cap is followed, as expected in a BN-SWNT.[3,32] A second NT's cut close to the tip of the new C-NT occurs straightforwardly. Thus, the recently constructed C structure confers further robustness to the BN-NT, preventing the collapse and destruction of the BN-NT as a result of the pressure effects, showing the "symbiotic" behavior of the two structures in the hybrid nanomaterial formation. Subsequently to the second BN-NT cut, the flat cap evolves to a crystalline conical tip, as previously shown for BN-MWNT in ref[29]

The diameter narrowing and eventual cut of the NT in the irradiation-induced processes stop once the hybrid double-walled nanostructure is fully formed, pointing out to the stability and robustness of the hybrid structure.

Knock-on damage and atomic displacement in C-NT are known to cause vacancies and other defects, which lead to a loss of the nanotube's graphitic structure.[15,31] In our experiments, during the shrinking and cutting of the NT, the formation of amorphous or disordered phases was not observed. In previous works, the irradiation experiments were carried out above 200 °C[15,31] to maintain the crystalline structure of the C-SWNT. In the case of C-NS, the damage annealing removes the point defects introduced by the electron beam irradiation. Irradiation-induced thermal effects in nanometer-thick materials are usually neglected,[31] and particularly in the case of good thermal conductors carbonaceous NS. However, these effects play here a prominent role. Paradoxically, the presence of the BN-NT and the subsequent limitation of the thermal conduction or heat dissipation allow the transformation of the C material. It has been proposed that the thermal conductivity of BN-MWNT is higher than that of C-MWNT,[33] even when the thermal conductivity of an h-BN structure is several times smaller than in graphene. This difference between BN-NT and h-BN was justified by the absence of dislocations in the NT. In the current case the irradiation on the BN-SWNT yields the formation of dislocations which justify a low thermal conductivity. This explains why the temperature reached in this hybrid system during the irradiation may be higher than the necessary for vacancy or divacancy diffusion in BN.[27] This confers an extraordinary stability to the NT and anneals the defects in BN and C nanotubes walls. It is worth to emphasize that

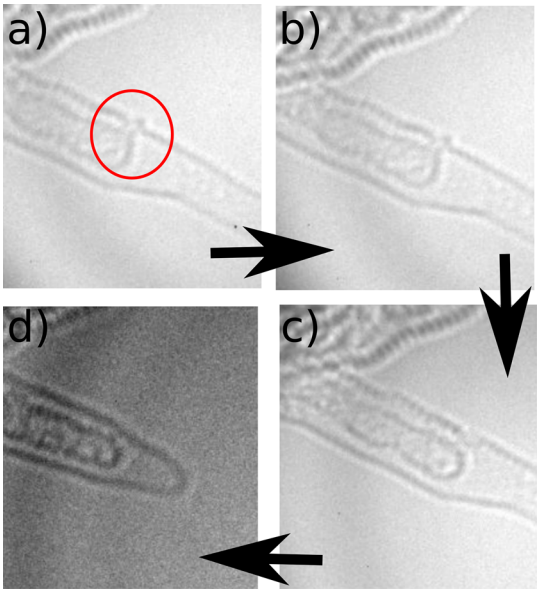

Figure 5. Four-frame sequence displaying the self-reparation process of a defected BN-NT sidewall in contact with hosted C-NT tip.

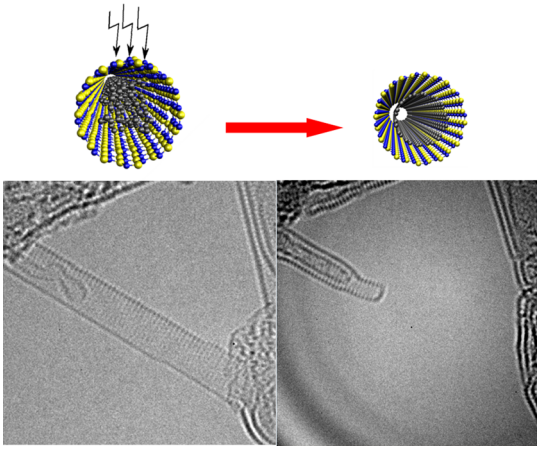

Figure 6. (a) Electronic band structure of a double-walled hybrid nanotube formed by a inner (7,7) C-NT concentric to a (12,12) BN-NT. (b) Electronic band structure of a single-walled (7,7) C-NT. (c) Cross-sectional view of the concentric nanotubes.

heating on the BN-NTs is mainly due to the ohmic dissipation of the irradiated electrons as a consequence of both their insulating electronic structure and presence of defects rather than an external source of heat.

Another interesting phenomenon occurring during the irradiation process is the formation of an atomic-scale bridge between the C-NT tip and the outer BN wall, and the subsequent reparation of the defect on both materials, see Figures 2, 3, 5 and in the Video S1 (provided in Supporting Information). Figure 5 displays in a four-frame sequence this process. A defect at the BN-NT surface enhances the C-BN interaction by establishing a connection between both tubes which can be related to thermal and pressure events such as the

evaporation of some C atoms and more likely the injection of B and/or N atoms inside of the NT.[15]

We suggest that the encapsulation of C-NT within a BN matrix ensures the fabrication of pure C-NTs protected from any source of environmental contamination that might alter their intrinsic electronic properties. First-principles calculations were performed to show that the hyperconjugated properties of the π-orbital network of the graphitic structure are not modified upon confinement within the BN hexagonal tubular lattice. Two concentric honeycomb lattices separated by the typical graphitic van der Waals distance of 3.3 Å are represented by a (7,7) C-NT coaxially hosted by a (12,12) BN-NT. The electronic band structure plotted in Figure 4a shows that the electronic states of both nanotubes do not interact with each other as demonstrated by the lack of band gap opening (bands hybridization) or modifications of the band dispersion. As a matter of fact, the removal of the external BN shell does not have major influence on both the distribution and the dispersion of the C-NT states, as shown by comparison with Figure 6b, which represents the band diagram of a pristine (7,7) C-NT.

CONCLUSION

We have *in situ* monitored by HRTEM the catalyst-free formation *via* electron-irradiation at room temperature and low vacuum of crystalline carbon nanotubes within single- and multiwalled boron nitride nanotubes. The transformation of BN-NT and the crystallization process undergone by the C atoms encapsulated within the BN-NT matrix upon irradiation were studied. We unveiled the physical mechanisms that led to the shrinking, cutting, and restructuration of the BN-NT to conclude that they are intimately related to the geometric and electronic configuration of constituent atoms. The BN-NT was observed to perform as a container, protective-cage, and template for the C material, which, in turns, confers robustness to the hybrid-structure. The two-phased heterostructure benefits from the complementary properties of the C and BN materials. Finally, we have illustrated that electron-irradiation is an effective pathway to construct BNC hybrid nanostructures in a controlled manner with potential applications in the fabrication of electronic devices in which the conducting channel remains independent and protected from any external perturbation.

MATERIALS AND METHODS

Experimental Techniques. The BN-NTs, having a relatively constant diameter of the order of less than 2 nm and good crystalline quality, were prepared by laser vaporization and have been thoroughly characterized by TEM (high resolution, electron diffraction and EELS) and Raman spectroscopy.[24,28,34,35] Most of the nanotubes ($\approx$ 80%) are single-walled (SW), but the samples also contain multiwalled (MW) NT, mainly double-walled (DW).

All the TEM studies were developed using two different FEI Titan microscopes, working at 80 keV to ensure a good control of the irradiation damage. HRTEM imaging was performed at room temperature, and in the microscope column vacuum, the pressure was in the order of 10^{-5} Pa. HRTEM images were acquired in an image corrected FEI Titan Cube 60-300 microscope. STEM imaging and spatial-resolved electron energy loss spectroscopy (SR-EELS) measurements were performed on probe-corrected STEM FEI Titan Low-Base 60-300 (fitted with a X-FEG gun and Cs-probe corrector (CESCOR from CEOS GmbH)). The sequence of images was recorded with an exposure time of 0.55 s and binning the pixels twice (1024 $\times$ 1024 pixel) to increase the contrast without increasing the exposure time. To obtain the electron dose, the flux calibration was performed using one image (1 s exposure time) taken without the sample in the beam. The dose was calculated by taking the ratio of the added number of electrons on the CCD camera and the area. EEL spectra were recorded using the spectrum-imaging mode[28,36] in a Gatan GIF Tridiem 865 ESR spectrometer. The convergent semiangle was of 25 mrad, the collection semiangle was of 80 mrad, and the energy resolution was $\approx$1.2 eV. Note that no hydrocarbon contamination depositions has been observed in any of all these (S)TEM experiments. Samples for TEM characterization were prepared by sonication of a small amount of powder in ethanol absolute. The dispersions were placed dropwise onto holey carbon grids.

Simulations. The geometry optimizations and electronic structure calculations were performed with the SIESTA code.[37,38] A double-ζ polarized basis set within the local density approximation approach for the exchange-correlation functional was used. Atomic positions were relaxed with a force tolerance of 0.01 eV/Å. The integration over the Brillouin zone was performed using a Monkhorst sampling of 1 $\times$ 1 $\times$ 64 k-points for the primitive armchair unit cell. The radial extension of the orbitals had a finite range with a kinetic energy cutoff of 50 meV. The numerical integrals were computed on a real space grid with an equivalent cutoff of 300 Ry.

Conflict of Interest: The authors declare no competing financial interest.

Acknowledgment. The TEM measurements were performed in the Laboratorio de Microscopías Avanzadas (LMA) at the Instituto de Nanociencia de Aragón (INA) - Universidad de Zaragoza (Spain). R.A. acknowledges funding from grants 165-119 and 165-120 from U. de Zaragoza and from ARAID foundation. The research leading to these results has received funding from the European Union Seventh Framework Program under Grant Agreement 312483 - ESTEEM2 (Integrated Infrastructure Initiative - I3). A.L.-B. gratefully acknowledges the computing resources provided on the Blues compute cluster operated by the Laboratory Computing Resource Center at Argonne National Laboratory. Work at Argonne is supported by DOE-BES under Contract No. DE-AC02-06CH11357. A.L.-B. acknowledges Glue funding from DOE (FWP#70081).

Supporting Information Available: HRTEM images of the hybrid DW-NT; high resolution *in situ* TEM movie showing the structural evolution of the disordered carbon nanostructure contained inside a BN-NT upon electron beam irradiation. This material is available free of charge *via* the Internet at http://pubs.acs.org.

REFERENCES AND NOTES

1. Shulaker, M. M.; Hills, G.; Patil, N.; Wei, H.; Chen, H.-Y.; PhilipWong, H.-S.; Mitra, S. Carbon Nanotube Computer. *Nature* **2013**, *501*, 526–530.

2. Loiseau, A.; Launois, P.; Petit, P.; Roche, S.; Salvetat, J.-P.; , Eds. *Understanding Carbon Nanotubes from Basics to Applications*; Series: Lecture Notes in Physics; Springer: New York, 2006; Vol. 677.
3. Arenal, R.; Blase, X.; Loiseau, A. Boron-Nitride and Boron-Carbon Nitride Nanotubes: Synthesis, Characterization and Theory. *Adv. Phys.* **2010**, *59*, 101–179.
4. Golberg, D.; Bando, Y.; Tang, C. C.; Zhi, C. Y. Boron Nitride Nanotubes. *Adv. Mater.* **2007**, *19*, 2413–2432.
5. Liu, Z.; Gong, Y.; Zhou, W.; Ma, L.; Yu, J.; Idrobo, J. C.; Jung, J.; MacDonald, A. H.; Vajtai, R.; Lou, J.; Ajayan, P. M. Ultrathin High-Temperature Oxidation-Resistant Coatings of Hexagonal Boron Nitride. *Nat. Commun.* **2013**, *4*, 2541.
6. Ayala, P.; Arenal, R.; Loiseau, A.; Rubio, A.; Pichler, T. The Physical and Chemical Properties of HeteroNanotubes. *Rev. Mod. Phys.* **2010**, *82*, 1843–1885.
7. Liu, A. C. Y.; Arenal, R.; Montagnac, G. *In Situ* Transmission Electron Microscopy Observation Of Kev-Ion Irradiation of Single-Walled Carbon and Boron Nitride Nanotubes. *Carbon* **2013**, *62*, 248–255.
8. *B-C-N Nanotubes and Related Nanostructures*; Yap, Y. K., Ed.; Springer: Dordrecht, 2009.
9. Enouz, S.; Stephan, O.; Cochon, J. L.; Colliex, C.; Loiseau, A. C-BN Patterned Single-Walled Nanotubes Synthesized by Laser Vaporization. *Nano Lett.* **2007**, *7*, 1856–1862.
10. Arutyunyan, N. R.; Arenal, R.; Obraztsova, E. D.; Stephan, O.; Loiseau, A.; Pozharov, A. S.; Grebenyukov, V. V. Incorporation of Boron and Nitrogen in Carbon Nanomaterials and Its Influence on Their Structure and Opto-Electronical Properties. *Carbon* **2012**, *50*, 791–799.
11. Arenal, R.; Wang, M. S.; Xu, Z.; Loiseau, A.; Golberg, D. Young Modulus, Mechanical and Electrical Properties of Isolated Individual and Bundled Single-Walled Boron Nitride Nanotubes. *Nanotechnology* **2011**, *22*, 265704.
12. Rubio, A.; Corkill, J. L.; Cohen, M. L. Theory of Graphitic Boron Nitride Nanotubes. *Phys. Rev. B* **1994**, *49*, 5081–5084.
13. Blase, X.; Rubio, A.; Louie, S. G.; Cohen, M. L. Stability and Band Gap Constancy of Boron-Nitride Nanotubes. *Europhys. Lett.* **1994**, *28*, 335–340.
14. Arenal, R.; Stephan, O.; Kociak, M.; Taverna, D.; Loiseau, A.; Colliex, C. Electron Energy Loss Spectroscopy Measurement of the Optical Gaps on Individual Boron Nitride Single-Walled and Multiwalled Nanotubes. *Phys. Rev. Lett.* **2005**, *95*, 127601.
15. Krasheninnikov, A. V.; Nordlund, K. N. Ion and Electron-Irradiation-Induced Effects in Nanostructured Materials. *J. Appl. Phys.* **2010**, *107*, 071301.
16. Terrones, M.; Banhart, F.; Grobert, N.; Charlier, J. C.; Terrones, H.; Ajayan, P. M. Molecular Junctions by Joining Single-Walled Carbon Nanotubes. *Phys. Rev. Lett.* **2002**, *89*, 075505.
17. Terrones, M.; Terrones, H.; Banhart, F.; Charlier, J. C.; Ajayan, P. M. Coalescence of Single-Walled Carbon Nanotubes. *Science* **2000**, *288*, 1226–1229.
18. Rodriguez-Manzo, J.; Terrones, M.; Terrones, H.; Kroto, H.; Sun, L.; Banhart, F. *In Situ* Nucleation of Carbon Nanotubes by the Injection of Carbon Atoms into Metal Particles. *Nat. Nanotechnol.* **2007**, *2*, 307.
19. Mickelson, W.; Aloni, S.; Han, W.-Q.; Cumings, J.; Zettl, A. Packing C60 in Boron Nitride Nanotubes. *Science* **2003**, *300*, 467–470.
20. Golberg, D.; Bando, Y.; Fushimi, K.; Mitome, M.; Bourgeois, L.; Tang, C. C. Nanoscale Oxygen Generators: MgO_2-Based Fillings of BN Nanotubes. *J. Phys. Chem. B* **2003**, *107*, 8726–8729.
21. Smith, B.; Luzzi, D. Electron Irradiation Effects in Single Wall Carbon Nanotubes. *J. Appl. Phys.* **2001**, *90*, 3509.
22. Borrnert, F.; Avdoshenko, S. M.; Bachmatiuk, A.; Ibrahim, I.; Buchner, B.; Cuniberti, G.; Rummeli, M. H. Amorphous Carbon under 80 kV Electron Irradiation: A Means to Make or Break Graphene. *Adv. Mater.* **2012**, *24*, 5630–5635.
23. Kurasch, S.; Kotakoski, J.; Lehtinen, O.; Skakalova, V.; Smet, J.; Krill, C. E., III; Krasheninnikov, A. V.; Kaiser, U. Atom-by-Atom Observation of Grain Boundary Migration in Graphene. *Nano Lett.* **2012**, *12*, 3168–3173.
24. Arenal, R.; Stephan, O.; Cochon, J.; Loiseau, A. Root-Growth Mechanism of Single-Walled Boron Nitride Nanotubes *via* Laser Vaporization Technique. *J. Am. Chem. Soc.* **2007**, *129*, 16183–16189.
25. Zobelli, A.; Gloter, A.; Ewels, C. P.; Seifert, G.; Colliex, C. Electron Knock-On Cross Section of Carbon and Boron Nitride Nanotubes. *Phys. Rev. B* **2007**, *75*, 245402.
26. Cosslett, V. E. Radiation Damage in the High Resolution Electron Microscopy of Biological Materials: A Review. *J. Microsc.* **1978**, *113*, 113.
27. Zobelli, A.; Gloter, A.; Ewels, C. P.; Colliex, C. Shaping Single Walled Nanotubes with an Electron Beam. *Phys. Rev. B* **2008**, *77*, 045410.
28. Arenal, R.; De la Pena, F.; Stephan, O.; Walls, M.; Tence, M.; Loiseau, A.; Colliex, C. Extending the Analysis of EELS Spectrum-Imaging Data, from Elemental to Bond Mapping in Complex Nanostructures. *Ultramicroscopy* **2008**, *109*, 32–38.
29. Celik-Aktas, A.; Stubbins, J. F.; Zuo, J. M. Electron Beam Machining of Nanometer-Sized Tips from Multiwalled Boron Nitride Nanotubes. *J. Appl. Phys.* **2007**, *102*, 024310.
30. Sun, L.; Banhart, F.; Krasheninnikov, A. V.; Rodriguez-Manzo, J.; Terrones, M.; Ajayan, P. M. Carbon Nanotubes as High-Pressure Cylinders and Nano-Extruders. *Science* **2006**, *312*, 1199–1202.
31. *In Situ Electron Microscopy at High Resolution*; Banhart, F., Ed.; World Scientific Publishing Company: Hackensack, NJ, 2008.
32. Loiseau, A.; Willaime, F.; Demoncy, N.; Schramchenko, N.; Hug, G. Boron Nitride Nanotubes. *Carbon* **1998**, *36*, 743–752.
33. Golberg, D.; Bando, Y.; Kurashima, K.; Sato, T. Synthesis and Characterization of Ropes Made of BN Multiwalled Nanotubes. *Scripta Mater.* **2001**, *44*, 1561–1565.
34. Arenal, R.; Kociak, M.; Loiseau, A.; Miller, D. J. Determination of Chiral Indices of Individual Single- and Double-Walled Boron Nitride Nanotubes by Electron Diffraction. *Appl. Phys. Lett.* **2006**, *89*, 073104.
35. Arenal, R.; Ferrari, A. C.; Reich, S.; Wirtz, L.; Mevellec, J.-Y.; Lefrant, S.; Rubio, A.; Loiseau, A. Raman Spectroscopy of Single-Wall Boron Nitride Nanotubes. *Nano Lett.* **2006**, *6*, 1812–1816.
36. Jeanguillaume, C.; Colliex, C. Spectrum-Image—The Next Step in Eels Digital Acquisition and Processing. *Ultramicroscopy* **1989**, *28*, 252–257.
37. Ordejon, P.; Artacho, E.; Soler, J. M. Self-Consistent Order-N Density-Functional Calculations for Very Large Systems. *Phys. Rev. B* **1996**, *53*, R10441–4.
38. Nakanishi, R.; Kitaura, R.; Warner, J. H.; Yamamoto, Y.; Arai, S.; Miyata, Y.; Shinohara, H. Thin Single-Wall BN-Nanotubes Formed Inside Carbon Nanotubes. *Sci. Rep.* **2013**, *3*, 1385.